GODDARD
GRANT
IN-35-CR
31

REPORT TO THE

NATIONAL AERONAUTICS AND SPACE ADMINISTRATION

- GODDARD SPACE FLIGHT CENTER -

FINAL STATUS REPORT

p. 15

for

GRANT NAG 5-1332

DESIGN, PERFORMANCE EVALUATION, AND INVESTIGATION OF THE THEORETICAL CAPABILITIES OF THE NASA MILLIMETER-WAVE IMAGING RADIOMETER (MIR)

A.J. Gasiewski (Principal Investigator)
D.M. Jackson

Covering the period from

March 1, 1990 to February 28, 1991

Submitted by:

Professor Albin J. Gasiewski
School of Electrical Engineering
Georgia Institute of Technology
Atlanta, Georgia, 30332-0250
(404) 894-2934

NASA Technical Officer:

Dr. Robert F. Adler
Laboratory for Atmospheres/Code 612
NASA Goddard Space Flight Center
Greenbelt, MD 20771
(301) 286-9086

TABLE OF CONTENTS

INTRODUCTION

Progress by investigators at the Georgia Institute of Technology in the development of techniques for passive microwave retrieval of water vapor and precipitation parameters using millimeter- and sub-millimeter wavelength channels is reviewed. Channels of particular interest are in the tropospheric transmission windows at 90, 150, 220, and 340 GHz and centered around the water vapor lines at 183 and 325 GHz. Collectively, these channels have potential application in high-resolution mapping (e.g., from geosynchronous orbit), remote sensing of cloud and precipitation parameters, and retrieval of water vapor profiles. Both theoretical and experimental results to date are discussed.

The theoretical effort has consisted of radiative transfer modeling using the planar-stratified numerical model described in Gasiewski and Staelin (1990). The model incorporates scattering and absorption from liquid and frozen spherical Mie-scattering hydrometeors. Extremely High Frequency (EHF) and Submillimeter-Wave (SMMW) brightness temperatures have been calculated for a variety of hydrometeor scenarios in order to determine the sensitivity of such spectra to hydrometeor parameters and water vapor.

The experimental effort has been associated with the design of the NASA Goddard Millimeter-Wave Imaging Radiometer (MIR). This instrument, when operated on the NASA ER-2 high-altitude platform, will provide radiometric data necessary for evaluation of radiative transfer models and development of retrieval techniques. Georgia Tech involvement has included overall MIR performance simulation, development of receiver specifications, instrument layout, data acquisition system design, and radiometric calibration load characterization and design.

SUMMARY OF ACTIVITIES

Three categories of research by Georgia Tech investigators supported under this grant can be defined: 1) millimeter- and submillimeter wave radiative transfer modelling, 2) performance analysis and design of the Millimeter-wave Imaging Radiometer (MIR), and 3) numerical electromagnetic and thermal analysis of microwave blackbody calibration loads. Progress within each of these categories will be discussed.

1. Radiative transfer Modelling

An analysis of the potential uses of specific Extremely High Frequency (EHF: 30-300 GHz) and Submillimeter-Wave (SMMW: 300+ GHz) channels for passive meteorological remote sensing has been performed using an iterative numerical radiative transfer model (Gasiewski and Staelin, 1990). The initial results of this sensitivity analysis are described by Gasiewski (1990, see Appendix A). A more thorough elaboration will be available in forthcoming paper to be submitted to the IEEE Transactions on Geoscience and Remote Sensing. Reported here are the essential findings:

A) Clear-air water vapor profiling can be performed, in principle, equally well using SMMW channels at 325+\-1,3,7 and 220 GHz as has been demonstrated using channels at 183+\-1,3,7, and 166 GHz. The enhanced spatial resolution available at the higher frequencies using diffraction limited apertures of fixed size make these channels desirable. However, water profiling using the 325 and 220 GHz channels alone is expected to be more adversely affected by clouds.

B) Coincident observations at using both low and high frequency channel sets (i.e., 166, 183+\-1,3,7, and 220, 325+\-1,3,7 GHz) are expected to provide at least one additional observable degree of freedom useful for estimating cloud water content, and possibly, cloud top altitude. This degree of freedom can be seen in the difference between computed 183 and 325 GHz spectra, and is expected to contain information not available using only one of these two channel sets. The additional degree of freedom will

be related to cloud particle size and density, but is not expected to be monotonic in these parameters.

C) Non-precipitating clouds such as high-altitude cumulus and cirrus are detectable using a 340 GHz or 325+\- 9 GHz channel. At tropical latitudes, the ability to discriminate between water vapor fluctuations and non-precipitating clouds using either of these SMMW channels is somewhat degraded relative to that at middle and polar latitudes, although these channels are still expected to be useful. Estimation of cloud parameters such as cirrus ice water content appears feasible, particularly within middle and polar latitudes. However, further work on the retrieval of cloud water using EHF and SMMW channels is needed.

D) The SMMW channels are somewhat more sensitive to clouds than EHF channels, although not as sensitive as IR channels. Overall, a 340-GHz channel will be less sensitive to storm structure and rain rate as one at 90-GHz, but more sensitive to thin ice canopies (<0.1g/m3 density), and should be particularly useful for detecting and mapping high-latitude snow and ice clouds. However, the sensitivity differences between a 90- and a 340-GHz channel are not expected to be nearly as significant as between a 90-GHz and an IR channel. In addition, the increased spatial resolution available at 340 GHz relative to 90 GHz (assuming diffraction limited apertures of equal size) is expected to benefit storm cell mapping.

Work is also in progress on the study of the observable modes in realistic EHF and SMMW brightness imagery of clouds and precipitation. Hydrometeor profiles are derived from volume reflectivity data of a convective storm observed by the CP-2 radar on July 11, 1986 during COHMEX. The hydrometeor profile data is used as input to the planar-stratified numerical radiative transfer model, which subsequently produces high-resolution (approximately 1 km spot size) brightness imagery.

A Karhunen-Loueve (or principal components) decomposition (Gasiewski and Staelin, 1989) is being implemented to reduce the complexity of the brightness spectra. This operation allows the sensitivity of the spectra to

meteorological parameters to be more easily studied. Using EHF and SMMW spectra, observable modes related to the amount of water and the ice size distribution are expected, but have not yet been ascertained. Moreover, these modes would be dependent on the spatial resolution of the imagery. To simulate satellite-based observations, the high-resolution brightness images are to be convolved with appropriate antenna gain patterns, and white observation noise will be added. The observable modes in these blurred, noisy images will be representative of what can be obtained from space-based passive imagers.

2. Performance Analysis and Design of the MIR

The most important activity to date has been the design of the MIR. Aircraft data from this instrument will be indispensable for clear-air EHF and SMMW radiative transfer and water vapor and precipitation sounding studies. Georgia Tech involvement has included overall MIR performance simulation, development of receiver specifications, instrument layout, data acquisition system design, and radiometric calibration load characterization and design.

Our clear-air radiative transfer calculations suggest that the channel specifications in Table 1 should be used to achieve reasonably uniform sampling of the vertical water vapor profile. It is noted that the channel set 90, 166, and 183+\-1,3,7 GHz exhibits a series of weighting functions with more uniformly-spaced peak-altitudes than the channel set 90, 150, and 183+\-1,3,7 GHz. Thus, it is expected that the former set (using 166-GHz) will be somewhat more useful for water vapor profile retrieval then the latter set (using 150-GHz). In addition, the 166-GHz channel lies in a band currently allocated for passive Earth remote sensing. As currently envisioned, the MIR will have a channel at 150 GHz (rather than 166 GHz) to coincide with a proposed Advanced Microwave Sounding Unit (AMSU) channel. This compromise will cause a slight reduction in scientific merit, particularly in the ability to experimentally assess any advantages in using either 166 or 150 GHz. However, it will allow coincident aircraft and AMSU satellite data to be immediately compared.

In order to simulate the in-flight performance on board the ER-2 aircraft, a spreadsheet program was written which allows various instrument parameters (e.g., antenna beamwidth, receiver noise figure, etc.) to be adjusted. The overall effects of these adjustments on many other dependent parameters (e.g., scan rate, instrument resolution, data rate, etc.) is immediately displayed. This program has been useful in optimizing the design of the MIR subject to the constraints of the ER-2 platform, the receiver noise figures, the channel frequencies, and other parameters. As currently envisioned, the MIR will have 3.5-degree antenna beamwidths for each channel. A spreadsheet printout listing this and other dependent and independent parameters is shown in Fig. 1.

The MIR will consist of two units: 1) the scanhead, and 2) the data acquisition/control and power system (Fig. 2). The scanhead will house the receivers, calibration loads, scanning mirror and motor, and load temperature sensors and regulators, IF and video electronics, and A/D and D/A converters. In order to minimize scanhead weight, the MIR will be a total power radiometer design. The data acquisition system will consist of a computer with floppy drive and cartridge tape mass storage unit. In order to retain an acceptable dynamic range and temperature resolution (400 K and 0.1 K, respectively) in the presence of inevitable receiver gain and offset fluctuations, an offset compensation circuit is being designed by Georgia Tech. Optoisolation of the analog module will be employed to decrease ground-loop noise susceptibility. The power module is to be designed yet, but will house all circuit breakers, indicators, DC-to-DC converters, and will function as the aircraft interface.

The implementation of a 325/340 GHz receiver on the MIR has been of high priority. We are currently in favor of a double-balanced Schottky diode mixer design, with a subharmonically-pumped local oscillator (LO) Gunn diode source. The LO frequency will be 162.5 GHz; the source will be replaceable with a 170 GHz Gunn oscillator for observations at 340 GHz. Waveguide, as opposed to quasi-optical diplexing seems more practical, although we are reviewing a single-ended quasi-optical Schottky design. Pending acquisition of funds, we plan to request bids for the 325/340 GHz

receiver during March, 1991. The receiver should be available for testing and integration before 1992.

3. Numerical Analysis of Microwave Blackbody Calibration Loads

To accurately calibrate the MIR, the calibration load total reflectivity needs to be less than 1%, and known to better than 0.1%. Manufacturer's specifications typically provide only the specular component of the reflectivity, which is thought to be substantially less than the total reflectivity. In order to refine our estimates of the total reflectivity, we are investigating the scattering of an incident plane wave from a calibration load modelled as a lossy periodic wedge grating.

One approach we are using is close to that described by Moharam and Gaylord (1982), in which the grating is partitioned into a number of thin planar slab gratings (see Appendix B). Within each slab the electromagnetic field can be decomposed into Floquet harmonics. A set of coupled wave equations is subsequently developed to relate the harmonics in adjacent slabs. A computer program based on this technique has been implemented, although a more economical matrix inversion method is yet needed for practical applications. Another approach that we are investigating is based on the periodic Green's function (Gasiewski, et al, 1991).

We have also analyzed the steady state thermal distribution in periodic wedge and pyramid calibration load structures using thermally conductive plate and rod (respectively) models. Initial results suggest that the temperature profiles within either wedge- or pyramid-type loads will be quite similar (for comparable height-to-pitch ratios), and hence either of these structures are equally acceptable for use as calibration loads in a dissipative (i.e., non-equilibrium) thermal environment.

CONCLUSIONS AND PLANS FOR FUTURE WORK

EHF and SMMW radiative transfer calculations have been carried out for hydrometeor-laden tropical, mid-latitude, and polar atmospheres. The results suggest that SMMW channels at 325 and 340 GHz offer significant potential for passive meteorological remote sensing, and experimental confirmation using aircraft observations at these frequencies is urged. The main findings have been enumerated in the previous section, and will be discussed in detail in a forthcoming publication.

The Karhunen-Loueve rank reduction analysis using simulated EHF and SMMW brightness imagery provides a quantitative method of determining the meteorological information content of passive microwave spectra observed using selected channel sets. Future plans include the use of more realistic hydrometeor profiles derived from a numerical cloud evolution model (the NASA Goddard Cumulus Ensemble - GCE), as described by Tao et al (1987). We also plan to investigate the effects of an antenna pattern deconvolution operator to enhance the resolution of satellite-based imagers. Under separate funding, the planar-stratified radiative transfer model is currently being upgraded to describe aspherical hydrometeor distributions. This capability will be useful in assessing the sensing potential of polarized EHF and SMMW channels for cirrus parameter retrieval.

To date, we have provided assistance to NASA/GSFC in the mechanical and electrical design of the MIR. Georgia Tech's main responsibilities are the design of the data acquisition system, implementation of MIR software, and development of the 325/340 GHz receiver. The construction of most components of the MIR are the responsibility of NASA/GSFC. The earliest test flight will be during fall 1991, using only the channels up to 220 GHz. The 325/340 GHz channel is expected to be added in 1992. Particular attention is being given to the instrument calibration, load temperature measurement hardware, video circuitry, and overall system interference immunity.

The radiometric calibration load reflectivity analysis will be continued beyond this grant, although this study will be of tertiary importance relative to the MIR construction and the theoretical radiative transfer analysis. Ultimately, we plan to perform numerical calculations of the bistatic scattering coefficient of a lossy periodic grating based on coupled-wave and periodic Green's function approaches, and to verify these calculations against laboratory measurements using similar wedge-shaped calibration loads. The resulting numerical model will be useful for the absolute calibration of the MIR as well as in future calibration load designs, particularly those wideband loads. Current calibration load designs are highly empirical, and the manufacturers' load specifications are generally insufficient for accurate calibration.

REFERENCES

Gasiewski, A.J., and D.H. Staelin, "Statistical Precipitation Cell Parameter Estimation Using Passive 118-GHz O_2 Observations," J. Geophys. Res., 94, D15, 18367-18378, 1989.

Gasiewski, A.J., and D.H. Staelin, "Numerical Analysis of Passive Microwave O_2 Observations Over Precipitation", Radio Science, 25, 3, 217-235, 1990.

Gasiewski, A.J., "Numerical Sensitivity Analysis of Passive EHF Channels to Tropospheric Water Vapor and Precipitation", Proceedings of the 1990 International Geoscience and Remote Sensing Symposium, 855-858, University of Maryland, College Park, MD, May 20-24, 1990.

Gasiewski, A.J., D.M. Jackson, and A.F. Peterson, "Electromagnetic Scattering from Lossy Corrugated Surfaces: Application to Microwave Absorbers", submitted for presentation at the 1991 North American Radio Science Meeting and International IEEE/AP-S Symposium, University of Ontario, June 24-28, 1991.

Moharam, M.G., and T.K. Gaylord, "Diffraction Analysis of Dielectric Surface Relief Gratings", J. Opt. Soc. Am., 72, 10, 1385-1392, 1982.

Tao, W.K., J. Simpson, and S.T. Soong, "Statistical Properties of a Cloud Ensemble: A Numerical Study", J. Atm. Sci., 44, 21, 3175-3187, 1987.

TABLES AND FIGURES

Table 1. MIR Channel Specifications

Ch #	LO Freq (GHz)	IF1 Freq (MHz)	BW (MHz)
1	89.000	1000.0	1000.0
2	150.000	1000.0	1000.0 *
3	183.310	1000.0	1000.0
4	183.310	3000.0	2000.0
5	183.310	7000.0	2000.0
6	220.000	2000.0	2000.0
7	325.150	1000.0	1000.0
8	325.150	3000.0	2000.0
9	325.150	7000.0	2000.0
10	340.000	2000.0	2000.0

* Although a similar channel at 166.000 GHz would provide a more uniformly distributed set of weighting function peaks, 150.000 GHz was chosen to coincide with the channel specifications on current operational satellites.

NASA GSFC/Georgia Tech Millimeter-Wave Imaging Radiometer (MIR)
"Spreadsheet" Analysis of Expected Performance
A.J. Gasiewski

1/24/91

COMMON INSTRUMENT PARAMETERS:

---------Mechanical:			
Air velocity	210	m/sec	(ER-2)
Aircraft altitude	20	km	(ER-2)
Scan limits	50	+/-deg	(measured wrt nadir)
Scan time	2.87	sec	(minimum of all active channels to prevent undersampling)
Calibration time	0.70	sec	(hot cal, cold cal, and mirror-motion overhead time)
Load dwell time	0.15	sec	(time spent viewing each of two loads)
Motion time	0.40	sec	(time spent moving throughout calibration portion of scan)
Raster time	2.17	sec	(time spent observing raster)
Raster efficiency	75.6	%	(fraction of scan time on raster)
Scanner velocity	46.1	deg/sec	(measured during raster scan)
---------Raster Radiometric Data:			
Antenna temp (min)	0	K	(minimum expected)
Antenna temp (max)	400	K	(maximum expected)
R-data rate	530	S/sec	(maximum R-sampling rate during raster)
(R-sample time)	1.89	msec	(minimum R-A/D sampling period during raster)
R-samples per scan	1147	S	(radiometric samples during raster scan)
# R-A/D bits	12	#	(radiometric A/D converter)
R-range (high)	600	K	(high radiometric saturation level)
R-range (low)	-100	K	(low radiometric saturation level)
Rad resolution	0.17	K	(radiometric quantization error)
R-data per scan	13764	bits	(radiometric raster data only)
R-data block	13824	bits	(raster data block size)
---------Calibration Radiometric Data:			
C-samples per scan	158	S	(radiometric samples during calibration views)
# R-A/D bits	12	#	(radiometric A/D converter)
C-data per scan	1896	bits	(radiometric calibration data only)
C-data block	2048	bits	(calibration data block size)
---------Thermometric Data:			
# thermistors	16	#	(thermistor data stored once per scan)
Therm avg samples	32	S/scan	(# thermistor samples avereged per scan)
T-sample rate	731.4	S/sec	(maximum T-sampling rate during calibration time)
(T-sample time)	1.37	msec	(minimum T-A/D sampling period during calibration)
# T-A/D bits	12	#	(thermometric A/D converter)
T-range (high)	400	K	(high thermistor saturation level)
T-range (low)	200	K	(low thermistor saturation level)
Therm resolution	0.049	K	(thermometric quantization error)
T-data per scan	384	bits	(thermometric data only: mean and variance)
T-data block	512	bits	(thermistor data block size)
---------Miscellaneous Data:			
Time code length	128	bits	(coded IRIG-B time code, saved once per scan)
Status information	256	bits	(misc information)
Misc block	512	bits	(miscellaneous information data block size)
---------Data Storage:			
Total data: 1 scan	16896	bits	(total data per scan)
(same as above)	2112	Bytes	(")
(same as above)	33	blocks	(" ;each block=512 Bytes)
Storage capacity	200	MBytes	(total medium storage capacity)
Operating duration	75.4	hrs	(total instrument operating time on single disk)

Figure 1. MIR spreadsheet performance analysis.

SPECIFIC CHANNEL PARAMETERS:

Channel (designation):	1	2	3	4	5	6	7	8	9	10
Center (LO) freq (GHz)	90	166	183	183	183	220	325	325	325	340
(nominal wavelength, mm)	3.33	1.81	1.64	1.64	1.64	1.36	0.92	0.92	0.92	0.88
IF band center freq (MHz)	1000	1000	1000	3000	7000	2000	1000	3000	7000	2000
Bandwidth (MHz)	1000	1000	1000	2000	2000	2000	1000	2000	2000	2000
(IF, single conversion DSB superheterodyne										
Beamwidth (deg)	3.45	3.45	3.45	3.45	3.45	3.45	3.45	3.45	3.45	3.30
(3-dB)										
Spot sizes (km)										
(mid altitude, nadir)	0.60	0.60	0.60	0.60	0.60	0.60	0.60	0.60	0.60	0.58
(mid alt, extreme,long)	0.94	0.94	0.94	0.94	0.94	0.94	0.94	0.94	0.94	0.90
(mid alt, extreme,trans)	1.46	1.46	1.46	1.46	1.46	1.46	1.46	1.46	1.46	1.39
(surface, nadir)	1.20	1.20	1.20	1.20	1.20	1.20	1.20	1.20	1.20	1.15
(surface, extreme, long)	1.87	1.87	1.87	1.87	1.87	1.87	1.87	1.87	1.87	1.79
(surface, extreme, trans)	2.91	2.91	2.91	2.91	2.91	2.91	2.91	2.91	2.91	2.79
Aperture (cm)	7.20	3.90	3.54	3.54	3.54	2.94	1.99	1.99	1.99	1.99
(linear field taper assumed)										
Feedhorn dia (cm)	7.92	4.29	3.89	3.89	3.89	3.24	2.19	2.19	2.19	2.19
(aperture +10%)										
Maximum scan period (sec)	2.87	2.87	2.87	2.87	2.87	2.87	2.87	2.87	2.87	***
(uniform sampling at mid-alt, nadir)										
# Spots (effective)	29	29	29	29	29	29	29	29	29	30
Int time/spot (msec)	75	75	75	75	75	75	75	75	75	72
(effective)										
Receiver noise temp (K)	750	1000	1200	1200	1200	1500	4000	3500	4000	3500
(noise figure, DSB, dB)	5.55	6.48	7.11	7.11	7.11	7.90	11.70	11.16	11.70	11.16
Total power sensitivity (K)										
(maximum, antenna)	0.13	0.16	0.19	0.13	0.13	0.16	0.51	0.32	0.36	0.32
(minimum, antenna)	0.09	0.12	0.14	0.10	0.10	0.12	0.46	0.29	0.33	0.29
(nominal, cal load)	0.06	0.08	0.10	0.07	0.07	0.09	0.33	0.20	0.23	0.20
Time constants/spot (#)	2	2	2	2	2	2	2	2	2	2
Video time const (sec)	0.037	0.037	0.037	0.037	0.037	0.037	0.037	0.037	0.037	0.036
(1 pole lo-pass response)										
A/D oversampling factor	1.1	1.1	1.1	1.1	1.1	1.1	1.1	1.1	1.1	1.1
A/D sampling int (msec)	17.0	17.0	17.0	17.0	17.0	17.0	17.0	17.0	17.0	***
(samples/sec)	58.8	58.8	58.8	58.8	58.8	58.8	58.8	58.8	58.8	0.0
Total power quantization error (K rms)										
(maximum, antenna)	0.011	0.011	0.011	0.011	0.011	0.011	0.011	0.011	0.011	***
RMS radiometric and quantization error, for each spot (K)										
(maximum, antenna)	0.13	0.16	0.19	0.13	0.13	0.16	0.51	0.32	0.36	***

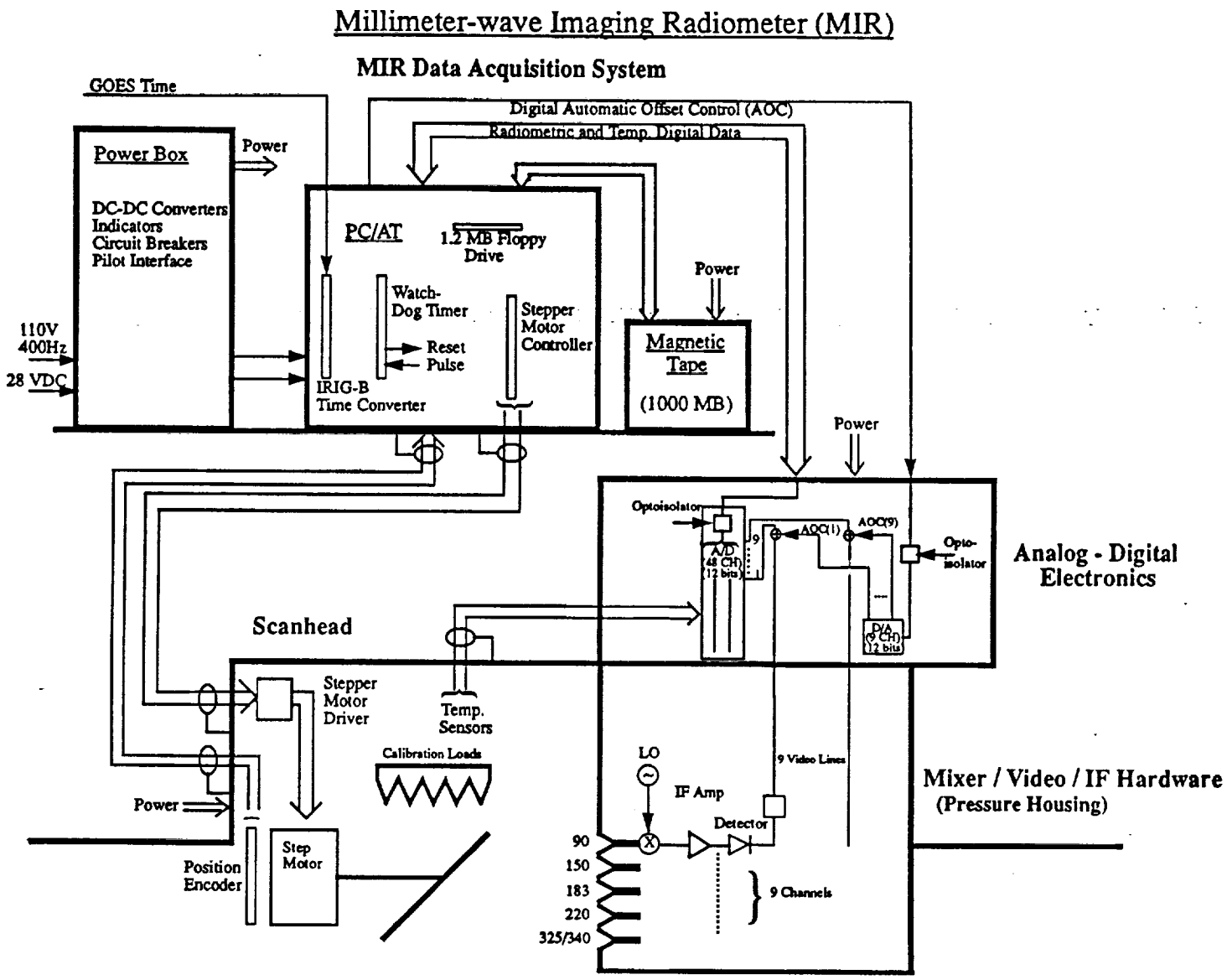

Figure 2. MIR block diagram, illustrating components in the scanhead and data acquisition system.